QUASIPARTICLE-VIBRATION COUPLING ON TOP OF SKYRME FUNCTIONALS: A SENSITIVITY STUDY*

G. Colò

Dipartimento di Fisica, Università degli Studi di Milano
via Celoria 16, 20133 Milano, Italy
and
INFN, Sezione di Milano, via Celoria 16, 20133 Milano, Italy

Z.Z. Li, Y.F. Niu

School of Nuclear Science and Technology, Lanzhou University
Lanzhou 730000, China
and
Frontiers Science Center for Rare Isotope, Lanzhou University
Lanzhou 730000, China

Received 20 December 2024, accepted 23 January 2025,
published online 10 April 2025

Our recent fully self-consistent model, that starts from QRPA on top of Skyrme–Hartree–Fock–Bogoliubov (SHFB) and includes the coupling between quasiparticles and vibrations, is discussed. We highlight the significant improvement of the results with respect to simple QRPA, and we focus on the sensitivity to the choice of a specific Skyrme functional.

DOI:10.5506/APhysPolBSupp.18.2-A8

1. Introduction

The study of nuclear Giant Resonances (GRs) has been, and still is, an active field of research [1]. This is, on the one hand, linked to the efforts to determine the nuclear Equation of State (EoS). In fact, GRs are collective modes that involve the coherent participation of many nucleons and, as such, they bring valuable information on the in-medium nucleon–nucleon (NN) interaction. While the nuclear Isoscalar Giant Monopole Resonance (ISGMR) has been shown to be sensitive to the nuclear incompressibility [2], the isovector modes have been intensively studied with the hope of understanding the isovector part of the NN Hamiltonian, the symmetry energy

* Presented at the 57$^{\rm th}$ Zakopane Conference on Nuclear Physics, *Extremes of the Nuclear Landscape*, Zakopane, Poland, 25 August–1 September, 2024.

as well as exotic nuclei and neutron stars [3]. The search for new, elusive nuclear excitation modes (toroidal excitation, to name only one) is actively pursued. At the same time, it would be desirable to find highly-selective ways to excite nuclei and obtain cleaner information about the quantum numbers and other properties of collective states. Vortex photons, that carry orbital angular momentum, have been proposed as a novel technique to selectively study isovector states [4].

GRs usually appear as broad bumps in the excitation function (*i.e.*, inelastic cross section as a function of the excitation energy). In addition to their peak energy, or average energy, they are characterised by a conspicuous width. The width amounts to several MeV, while typical excitation energies are in the range between 10 and 30 MeV. The standard understanding is that the width is either associated with coupling with more complex nuclear excitations that lie at similar energy as the resonance, or ultimately with the decay of the resonance by particle emission. However, this picture is still not fully understood. Measurements and/or calculations of the different decay channels are still scarce, although some few cases have been studied in the past. For instance, the balance between direct and statistical particle emission is still under debate.

The excitation of GRs is often described on the basis of one-particle–one-hole ($1p$–$1h$) excitations. This amounts to the standard Random Phase Approximation (RPA) theory that can be found in textbooks [5]. RPA is generalised to Quasiparticle RPA (QRPA) in the case of open-shell nuclei. RPA and QRPA cannot, as a rule, account for the whole GR width. They can describe the fragmentation of the resonance, or their coupling to residual $1p$–$1h$ states, which is often referred to as "Landau damping". By definition, they cannot describe the coupling of the GR with more complex configurations.

We have recently developed a fully self-consistent model that starts from QRPA on top of Skyrme–Hartree–Fock–Bogoliubov (SHFB), and includes the coupling with the most relevant configurations of the $2p$–$2h$ type: these are $1p$–$1h$ states plus another nuclear vibration or "phonon". These are also called "doorway states" in what follows. This wording has its origin in the fact that these states are the first step towards coupling with $3p$–$3h$ ... up possibly to a compound nucleus state where energy is statistically distributed among all possible degrees of freedom. In fact, it has been shown that our model (named Quasiparticle Vibration Coupling, or QPVC, model) is able to reproduce well the observed GR width. Our model has been originally introduced for charge-exchange GRs in Ref. [6] (*cf.* also [7] for a first version of the model without the pairing). More recently, in Ref. [8], the model has been applied to one of the most important non-charge-exhange GRs, the aforementioned ISGMR. Using our model, we have been able to show that we can extract a consistent value for the nuclear incompressibility, starting from measurements in different nuclei; this was not the case earlier, when simple QRPA was used and the value of incompressibility was inconsistent when extracted from either ^{208}Pb or Sn isotopes.

The present paper goes together with Ref. [9]. In this work, we have extended our analysis and considered the application of the self-consistent QPVC model to the Isovector Giant Dipole Resonance (IVGDR) and the Isoscalar Giant Quadrupole Resonance (ISGQR). In the current paper, we discuss the sensitivity of the QPVC results for ISGMR, IVGDR and ISGQR to the chosen Skyrme EDF. The paper is structured as follows. In Section 2, the formalism is briefly summarised. In Section 3, our results are shown and commented on before conclusions are drawn in Section 4.

2. Formalism

The formalism of our self-consistent QPVC model is illustrated in detail in our latest paper [9], and we provide only a brief sketch here.

We start from QRPA on top of fully self-consistent Skyrme HFB that is solved in the canonical basis as was done earlier in Ref. [10]. The creation operator of a QRPA state $|n\rangle$ reads

$$Q_n^\dagger = \sum_{a<b} X_{ab}^{(n)} \alpha_a^\dagger \alpha_b^\dagger - Y_{ab}^{(n)} \alpha_b \alpha_a \,, \tag{1}$$

where $\alpha^\dagger$ (α) are standard quasiparticle creation (annihilation) operators, while X and Y are the forward-going and backward-going QRPA amplitudes. In the QRPA+QPVC approach, the creation operator is generalised to include the doorway state contribution and reads

$$\mathcal{O}_\nu^\dagger = \sum_{a<b} \left(X_{ab}^{(\nu)} \alpha_a^\dagger \alpha_b^\dagger - Y_{ab}^{(\nu)} \alpha_b \alpha_a \right) + \sum_{a<b,n} \left(X_{abn}^{(\nu)} \alpha_a^\dagger \alpha_b^\dagger Q_n^\dagger - Y_{abn}^{(\nu)} Q_n \alpha_b \alpha_a \right) . \tag{2}$$

Having this ansatz for the operator, one can use the equation-of-motion method (in analogy to the standard QRPA) to determine the unknown amplitudes. The equation of motion reads

$$\langle \mathrm{QPVC}| \left[\delta\mathcal{O}_\nu, \left[H, \mathcal{O}_\nu^\dagger \right] \right] |\mathrm{QPVC}\rangle = E_\nu \langle \mathrm{QPVC}| \left[\delta\mathcal{O}_\nu, \mathcal{O}_\nu^\dagger \right] |\mathrm{QPVC}\rangle \,. \tag{3}$$

Here, ν labels the excited states and E_ν is the excitation energy with respect to the ground state $|\mathrm{QPVC}\rangle$ that is the vacuum of the QPVC annihilation operators $\mathcal{O}_\nu$ (for every ν). By introducing the conjugate operator $\mathcal{O}_\nu^\dagger$, and by equating its first-order variation to zero, one obtains QPVC equations that are similar to SRPA (*cf.*, *e.g.*, Ref. [11])

$$\begin{pmatrix} A_{ab,a'b'} & B_{ab,a'b'} & A_{ab,a'b'n'} & 0 \\ -B^*_{ab,a'b'} & -A^*_{ab,a'b'} & 0 & -A^*_{ab,a'b'n'} \\ A_{abn,a'b'} & 0 & A_{abn,a'b'n'} & 0 \\ 0 & -A^*_{abn,a'b'} & 0 & -A^*_{abn,a'b'n'} \end{pmatrix} \begin{pmatrix} X^{(\nu)}_{a'b'} \\ Y^{(\nu)}_{a'b'} \\ X^{(\nu)}_{a'b'n'} \\ Y^{(\nu)}_{a'b'n'} \end{pmatrix} = E_\nu \begin{pmatrix} X^{(\nu)}_{ab} \\ Y^{(\nu)}_{ab} \\ X^{(\nu)}_{abn} \\ Y^{(\nu)}_{abn} \end{pmatrix} . \tag{4}$$

We do not give the detailed expressions of the matrix elements here but the reader can see them in Ref. [9]. The key point is that the number of doorway states can be very large in the GR excitation energy region, so solving the latter equation may be hard or prohibitive. It is possible, instead, to use standard projection methods to project the QPVC equation (4) onto the Q_1 space spanned by the two quasiparticle excitations. The result is

$$\begin{pmatrix} A_{ab,a'b'} + W^{\downarrow}_{ab,a'b'}(E) & B_{ab,a'b'} \\ -B^*_{ab,a'b'} & -A^*_{ab,a'b'} - W^{\downarrow *}_{ab,a'b'}(-E) \end{pmatrix} \begin{pmatrix} X^{(\nu)}_{a'b'} \\ Y^{(\nu)}_{a'b'} \end{pmatrix} = E \begin{pmatrix} X^{(\nu)}_{ab} \\ Y^{(\nu)}_{ab} \end{pmatrix} , \tag{5}$$

where A and B are the QRPA matrices and the QPVC effects are encoded in the matrix $W^{\downarrow}$. The different Feynman diagrams contributing to the matrix elements of $W^{\downarrow}$ are depicted in Fig. 1. The so-called subtraction method is applied.

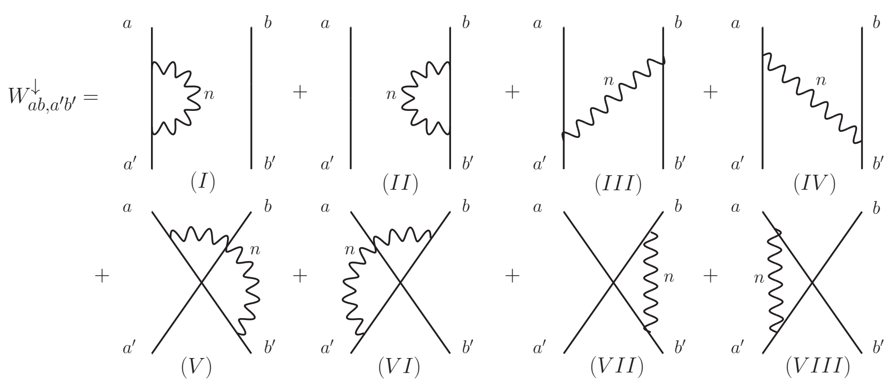

Fig. 1. The Feynman diagrams associated with the coupling between two-quasiparticles and the doorway states. See the main text.

The matrix in Eq. (5) is complex symmetric and the solutions form a biorthogonal basis. As a consequence, the strength function associated with the operator $\hat{O}_{\lambda\mu}$ is

$$S(E) = -\frac{1}{\pi} \mathrm{Im} \sum_{\mu\nu} \frac{\langle 0|\hat{O}_{\lambda\mu}|\nu\rangle^2}{E - \Omega_\nu + i\left(\frac{\Gamma_\nu}{2} + \eta\right)} . \tag{6}$$

Here, $\Omega_\nu - i\Gamma_\nu/2$ is the eigenvalue corresponding to the QPVC eigenstate $|\nu\rangle$. The details that are not discussed in this section can be found in Refs. [7–9, 12].

The effect of the coupling with doorway states, that is associated with $W^{\downarrow}$, is that of producing a shift of the GR peak and broadening it. These two effects are associated with the real and imaginary parts of $W^{\downarrow}$, respectively. The shift is towards lower energy, namely the QPVC strength function is peaked at lower energy than the QRPA one. We can understand this effect since the doorway states lie, on average, at higher energy than the GR. A specific example is shown in Fig. 2. In the case of the ^{120}Sn nucleus, and of the Skyrme interaction SV-K226, we display the energy shift ΔE (that is the difference between the QRPA and QPVC peaks) in the case of the ISGMR, IVGDR, and ISGQR. One can see that the shift is of the order of $\approx$ 1–1.5 MeV and is slightly larger for the dipole and quadrupole, as compared to the monopole case. The contribution from doorway states associated with phonons having different multipolarity J^π is also shown. The 3^- contribution is the largest but also 2^+, 4^+, and 5^- play an important role because low-lying collective states exist. This is not the case for 0^+ and 1^-, and this explains why these phonons contribute less.

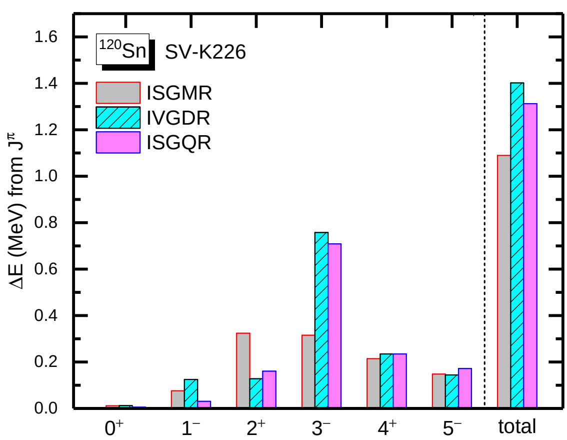

Fig. 2. Energy shift $\Delta E = E_{\rm QRPA} - E_{\rm QPVC}$ in a specific case, and breakdown of the contributions to it associated with different phonons. See the text for a short discussion.

3. Results

3.1. ISGMR

In Fig. 3, we show some of our results for the ISGMR, by using two different Skyrme EDFs that are SV-K226 and SkM*. These are, respectively, shown in the upper and lower panels. The three nuclei that have been considered are ^{120}Sn, ^{208}Pb, and ^{48}Ca. The first remark is that the QRPA curves in the different panels correspond to a set of discrete states that have been smeared out using Lorentzian functions having a width of 1 MeV. Even with this artificial width, QRPA does not reproduce the experimental ISGMR width. QPVC gives a good reproduction of the spreading width of the resonance, and this statement is not much interaction-dependent, if one compares the upper and lower panels. It should be emphasised that the three nuclei include two magic nuclei and a superfluid one, so the good reproduction of the strength function and its width is not particularly related to the magic or open-shell character of the nuclei under study, although pairing has to be included obviously in open-shell systems. The other remark is that the centroid energy is shifted from QRPA to QPVC, as we discussed in the previous section, but this shift is not so much interaction-dependent. The main difference between SV-K226 and SkM* is the centroid energy and this is already true at the QRPA level.

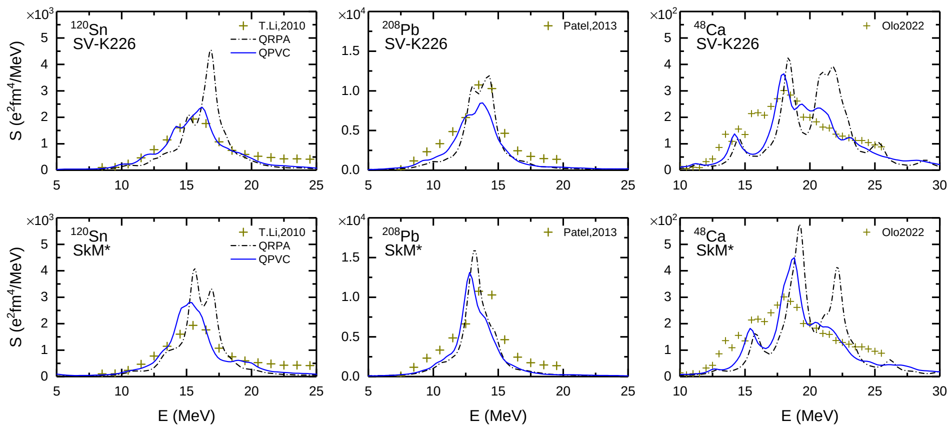

Fig. 3. Comparison between experimental data and theoretical QRPA and QPVC calculations in the case of the monopole strength. The experimental data are taken from Refs. [13–15].

To highlight this more clearly, in Fig. 4, we show, in the QPVC case, the results associated with the two interactions in the same plot. SkM* has a lower incompressibility (215 MeV) compared to SV-K226 (226 MeV). In ^{120}Sn and ^{208}Pb, one can clearly see that the centroid energy is lower when the incompressibility is lower. This is harder to be seen in ^{48}Ca, due to a larger amount of fragmentation of the monopole strength in this nucleus; however, the centroid energies calculated with SkM* and SV-K226 are, respectively, 19.89 MeV and 20.09 MeV, so the one associated with the lower incompressibility is indeed slightly lower.

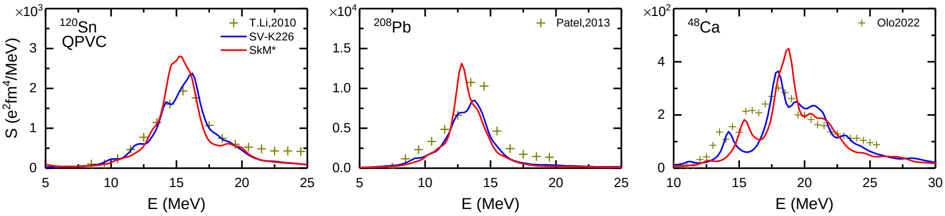

Fig. 4. The same as Fig. 3 but without the QRPA results, and with the QPVC results for the two EDFs in the same panel.

3.2. IVGDR

In the same way as in the previous subsection, we show here QRPA and QPVC results for the dipole strength. We employ three different Skyrme forces, and the three rows in Fig. 5 correspond to these three sets that are SV-K226, SkM*, and SAMi-T. The experimental data have a clear, smooth Lorentzian shape. The QRPA results (smeared by Lorentzians as in the monopole case) have, in most of the cases, double- or triple-peak structures that are not present in the data. The QPVC results are much closer to the

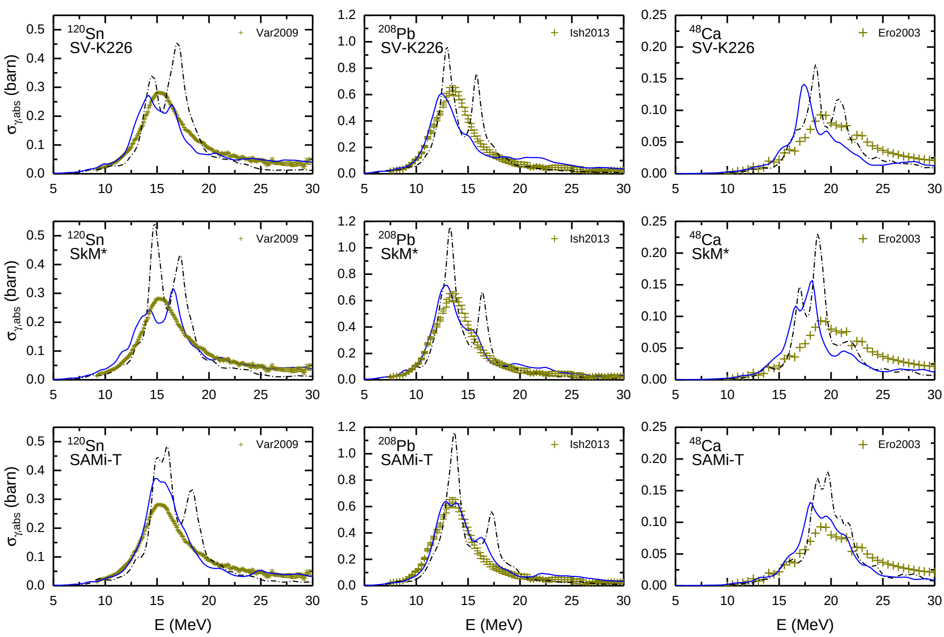

Fig. 5. Photoabsorbtion data compared with theoretical QRPA and QPVC calculations. The QRPA (QPVC) calculations are displayed by using the dash–dotted (full) lines. The experimental data, corresponding to the crosses, are taken from Refs. [16–18].

data, the artificial structures that are not in the data disappear in most of the cases, and the width is genuine and in good agreement with experiment. The centroid energy is the main feature that depends on the chosen interaction.

This is more clearly shown in Fig. 6 where, in the same way as above, we show the QPVC results associated with the different EDFs in the same plot. We have made an extensive search and found out that SAMi-T is providing the best description of IVGDR data in the nuclei that we have considered, among several EDFs that had been tried. The plots in Fig. 6 give an idea of the sensitivity of the results to the chosen Skyrme EDF.

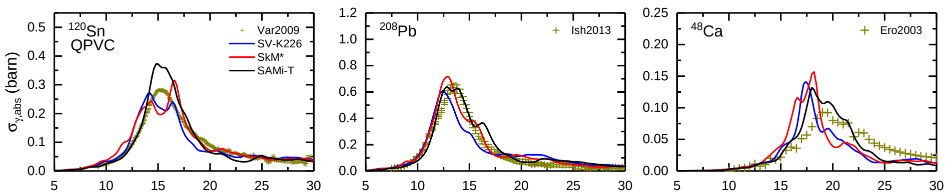

Fig. 6. The same as Fig. 5 but without the QRPA results, and with the QPVC results for the three EDFs in the same panel.

3.3. ISGQR

The results for the ISGQR, both in the QRPA and QPVC case, are shown in Fig. 7. Here, the energy shift and the broadening, when going from QRPA and QPVC, are even more evident than it was in the ISGMR and IVGDR study. The main ISGQR peak is very wide, and this agrees with

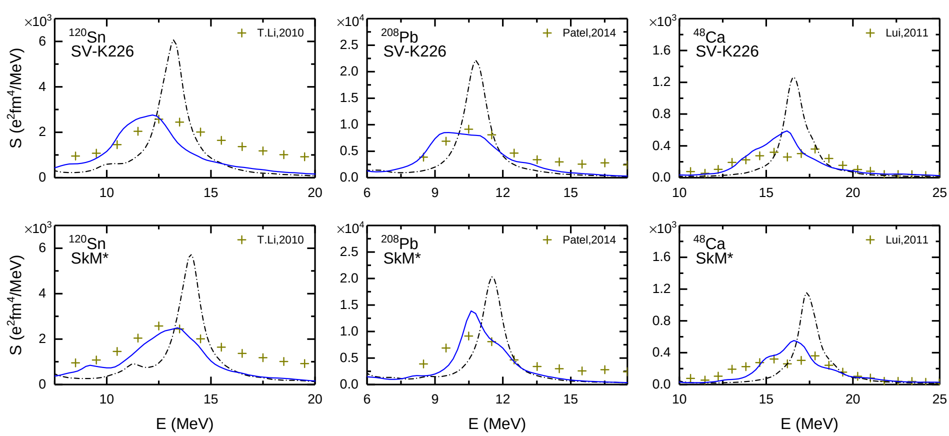

Fig. 7. Comparison between experimental data and theoretical QRPA and QPVC calculations in the case of the quadrupole strength. The experimental data are taken from Refs. [13, 19, 20].

the data from Refs. [13, 19, 20] (although the data of [13] are characterised by a significant amount of strength above the resonance region, and this is also true to some extent for the data from [20]).

Along the same spirit of our previous discussion, we show the QPVC results for the two interactions in the same panel in Fig. 8. The ISGQR energy has been known for some time to be sensitive, within (Q)RPA, to the effective mass: to be more precise, the energy should be correlated with $(m/m^*)^{1/2}$. We have performed a study of this dependence in our recent work [9], and extracted quantitative conclusions about the effective mass. Here, we use two EDFs, SkM*, and SV-K226, in order to show the sensitivity of the QPVC results to the choice of the EDF. In the quadrupole case, the results that better compare with experiment are those obtained by using SkM*.

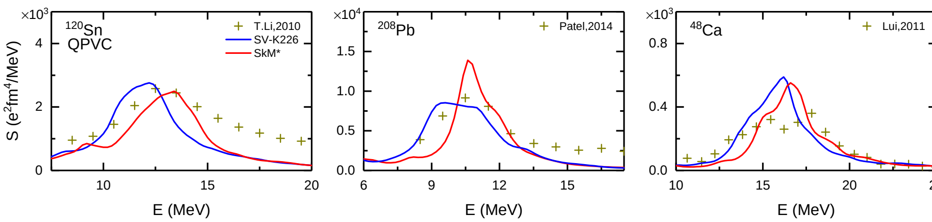

Fig. 8. The same as Fig. 7 but without the QRPA results, and with the QPVC results for the two EDFs in the same panel.

4. Conclusions

In the present work, we have sketched our recent QRPA+QPVC approach, which is a fully self-consistent model built on top of Skyrme-HFB. The model had been previously applied to charge-exchange states, while recently it has been used to study the ISGMR and solve the famous problem of the inconsistency between incompressibility values extracted from different nuclei. Here, we present results for ISGMR, IVGDR, and ISGQR, and focus on the sensitivity of the results to the choice of the EDF.

The QPVC results show a significant improvement with respect to QRPA and, in general, reproduce very well the width of the different GRs. With respect to QRPA, one does not only observe a broadening of the strength, associated with a good description of the resonance width, but also a systematic downward shift. Using ^{120}Sn as an example, we have compared the shifts associated with the different modes and the contribution of the doorway states associated with different phonons.

The problem which is left is the lack of a single EDF that can describe well the three resonances. For one of them, whether monopole, dipole, and quadrupole, we can find a good Skyrme EDF that reproduces the experimental data in various spherical nuclei, either magic or open-shell. The "universal" EDF is still to be found.

Z.Z. Li acknowledges the support of the China Postdoctoral Science Foundation under grant No. 2024M750047.

REFERENCES

[1] M.N. Harakeh, A. Woude, «Giant Resonances: Fundamental High-frequency Modes of Nuclear Excitation», *Oxford University Press*, 2001.

[2] U. Garg, G. Colò, *Prog. Part. Nucl. Phys.* **101**, 55 (2018).

[3] X. Roca-Maza, N. Paar, *Prog. Part. Nucl. Phys.* **101**, 96 (2018).

[4] Z.-W. Lu *et al.*, *Phys. Rev. Lett.* **131**, 202502 (2023).

[5] P. Ring, P. Schuck, «The Nuclear Many-Body Problem», *Springer-Verlag*, Berlin–Heidelberg–New York 2004.

[6] Y.F. Niu *et al.*, *Phys. Rev. C* **94**, 064328 (2016).

[7] G. Colò, N. Van Giai, P.F. Bortignon, R.A. Broglia, *Phys. Rev. C* **50**, 1496 (1994).

[8] Z.Z. Li, Y.F. Niu, G. Colò, *Phys. Rev. Lett.* **131**, 082501 (2023).

[9] Z.Z. Li, Y.F. Niu, G. Colò, *Phys. Rev. C* **110**, 064317 (2024).

[10] J. Terasaki *et al.*, *Phys. Rev. C* **71**, 034310 (2005).

[11] C. Yannouleas, *Phys. Rev. C* **35**, 1159 (1987).

[12] S. Shen, G. Colò, X. Roca-Maza, *Phys. Rev. C* **101**, 044316 (2020).

[13] T. Li *et al.*, *Phys. Rev. C* **81**, 034309 (2010).

[14] D. Patel *et al.*, *Phys. Lett. B* **726**, 178 (2013).

[15] S.D. Olorunfunmi *et al.*, *Phys. Rev. C* **105**, 054319 (2022).

[16] V. Erokhova *et al.*, *Izv. Akad. Nauk SSSR. Ser. Fiz.* **67**, 1479 (2003).

[17] V. Varlamov, B. Ishkhanov, V. Orlin, V. Chetvertkova, *Preprint MSU SINP* **3**, 847 (2009).

[18] V. Varlamov *et al.*, *Phys. At. Nuclei* **76**, 1403 (2013).

[19] Y.-W. Lui *et al.*, *Phys. Rev. C* **83**, 044327 (2011).

[20] D. Patel *et al.*, *Phys. Lett. B* **735**, 387 (2014).